Proceedings of MARTEC 2010
The International Conference on Marine Technology
11-12 December 2010, BUET, Dhaka, Bangladesh

INVESTIGATION OF THE RESPONSE OF A BOXED SHAPED FREE FLOATING BUOY IN REGULAR WATER WAVES

Muammer Din Arif[1], M. Rafiqul Islam[2], A. K. M. Sadrul Islam[3], Enaiyat Ghani Ovy[4]

[1]Industrial Lubricants Engineer
ExxonMobil, Bangladesh
M.Sc. (Mechanical Engineering)
Department of Mechanical & Chemical Engineering
Islamic University of Technology (IUT)
139, Rd: 1 (West), DOHS Baridhara, Dhaka, Bangladesh
Email: marif@mtu.edu

[2]Professor
Department of Naval Architecture and Marine Engineering
Bangladesh University of Engineering & Technology (BUET)
Dhaka: 1000, Bangladesh
Email: rafiqis@name.buet.ac.bd

[3] Professor
Department of Mechanical & Chemical Engineering
Department Head
Civil Engineering Department
Islamic University of Technology (IUT)
Board Bazar, Gazipur, Dhaka: 1704, Bangladesh
Email: sadrul@iut-dhaka.edu

[4]Lecturer
Department of Mechanical & Chemical Engineering
Islamic University of Technology (IUT)
Board Bazar, Gazipur, Dhaka: 1704, Bangladesh
Email: enaiyat_ovy@yahoo.com

ABSTRACT

The density, intermittency, and predictability of wave power make it the ideal renewable energy source for zero pollution electricity generation. A numerical analysis was carried out using Visual Studio FORTRAN 5.0, employing 3-D Sink Source Method, on a box shaped free floating buoy, in linear water waves. The motion responses (6 degrees of freedom) of the buoy were determined with the aid of a Boundary Element wire mesh, for given water depth (100m), wave incident angle (180º), and wave period (3 to 26 s). The main objective is to use the results to aid in the subsequent design of an Oscillating Water Column (OWC) Wave Energy Absorber. The FORTRAN algorithm calculated wave loads and buoy motions for each individual wave period input by the user. The program first determined the velocity potentials of the incident waves. This was subsequently used to compute the pressures and thus, forces and moments exerted by the incident waves, on the wetted surface of the buoy. From the calculated parameters, the various motions of the buoy i.e.: heave, surge, sway, roll, pitch, and yaw were found. Finally, the desired wave period(s) for optimal buoy motions were determined. It was found that the magnitudes of the motions of interest (heave, pitch, and surge) were the highest when the wave frequencies were in proximity of the buoy's natural frequencies. The buoy is a similitude of the full scale wave energy absorber. Thus, these results will be used in subsequent research, by the authors, involving the evaluation of the optimal performance of a Single Free-Floating Backward Bent Duct Buoy, housing an Oscillating Water Column and turbine--to generate electricity.

Keywords: *Wave Energy Absorber, Single Body Free Floating Buoy, Backward Bent Duct Buoy, Oscillating Water Column, Renewable Energy, Boundary Element Method, 3-D Sink Source Method, Numerical Model.*

1. INTRODUCTION

Sea and ocean wave energy has been gaining popularity as a viable and clean renewable energy source, namely for electricity generation. Duckers [1] stated that the potential world wave energy resource was similar in magnitude to that globally available from hydro-energy (2000 GW). He also discussed that waves are typically 2 to 3 times more powerful in deep offshore areas compared to coastal regions. The authors, accordingly, have modeled and determined the motion responses of a free floating buoy in waters of 100 m depth. A large amount of research and model-testing has been done with, offshore and coastal, wave energy convertors since the early 1970s. The research topics have been manifold: (1) characterization of wave energy resources, (2) theoretical and numerical analysis of the hydrodynamics of wave energy absorption, (3) design and construction of varied energy convertors, (4) the development of power take-off mechanisms (PTOs) such as: air and water turbines, power hydraulics, and linear electrical generators etc. Pioneers in this field include: McCormick [7], Shaw [8], and Masuda [6]. Masuda [6] was the first to develop a working

navigation buoy housing an Oscillating Water Column (OWC) which ran an air turbine [2], as shown in Figure 1.

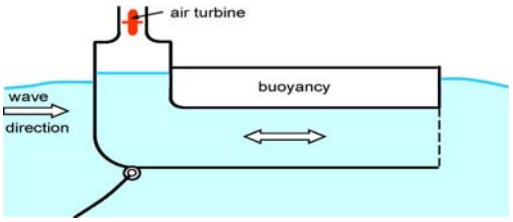

Figure 1. Schematics of a Backward Bent Duct Buoy (BBDB) Wave Energy Convertor

These buoys have been commercialized in Japan since 1965. The seminal work of Slater [9] also helped boost the worldwide interest in wave energy convertors. Presently, research and testing of wave energy convertors are underway in UK, Norway, Japan, India, Lisbon, Portugal, Greece, Denmark, Sweden, Canada, USA etc. From the standpoint of available technology and economy, wave energy convertors are most profitable for power generation in nations where other methods of electric power generation are costly or non-existent [1].

In the current research, the authors investigated the motion responses of a box-shaped buoy, in linear water waves, considering 6 degrees of freedom (DOF); namely: heave, surge, sway, pitch, roll, and yaw. Three of these degrees of freedom, heave, pitch, and surge, were considered important because these three motions are directly responsible for producing the oscillations in the water column of a wave energy convertor [1]. The complex hydrodynamic mathematical relations were solved and approximated using Finite Boundary Element and 3-D Sink Source methods. Both these methods have been perennially used in the design of ships and large offshore structures.

2. METHOD

2.1 Discussion

A free floating buoy in normal sea states has 6 DOF as shown in Figure 2. Heave, pitch, and surge are the most important motion modes for OWC generators housed in free floating buoys. Thus, the origin of these motions and the buoy's resonance behavior in these modes were analyzed in detail.

The incident waves impart forces and moments on the buoy which manifest as these 6 DOF. The induced motion is mainly linearly-excited motion [3].

High frequency motions are mostly caused by non-linear waves and transient effects such as 'ringing' and 'springing.' Similar non-linear effects, current, and wind forces also cause slow drift motions of the buoy. To counter such effects a mooring system is utilized as shown in Figure 1. Therefore, for the sake of simplification, the authors assumed a moored free floating buoy, which is buoyant in normal sea state and excited only by regular sinusoidal propagating waves.

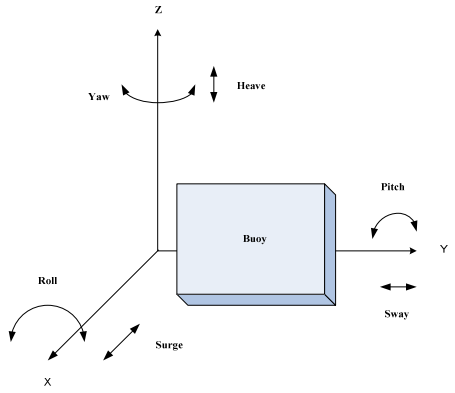

Figure 2. 6 DOF of Buoy

Hong et al. [4] did extensive numerical analysis on the motions of and drift forces on Backward Bent Duct Buoy (BBDB) OWC wave energy absorbers. Their model consisted of buoyancy module connected to a box housing the OWC. The OWC housing is submerged and connects to the sea water through a duct. In their research they utilized a numerical tank to approximate the pressure drop in the air chamber above the OWC, using linear wave theory.

Falcao [2] modeled a rectangular box-shaped buoy containing a PTO. He varied the linear damping coefficient of the PTO in order to determine the energy conversion efficiency of the buoy under normal sea states.

Faltinsen [3] used 2-D panel elements to discretize the wetted surface of a large rectangular box-shaped body in order to numerically evaluate sea loads on offshore structures.

All three of the above models: Hong et al. [4], Falcao [2], and Faltinsen [3], were used as guidelines and for validation of the results obtained by the authors.

2.1.1 Heave, Pitch, and Surge Motions

The typical BBDB housing an OWC has three types of resonance behaviors: (1) the resonance behavior of the OWC, (2) the coupled resonance motion, and (3) the uncoupled resonance motion for each DOF. The highest amplitudes of motions are attained when the wave period nearly equals one of the buoy's aforementioned natural period types. This fact is very important in the effective design of the buoy, since, greater response motion amplitude means greater extraction of wave energy for power generation. The numerical buoy model used by the authors lacks an OWC and thus, the first type of resonance behavior was absent.

The uncoupled and undamped natural periods for the three motions (heave, pitch, and surge) can be determined from the following general formula (refer to Table 1 for explanation of the variables):

$$T_{ni} = 2\pi \{(M_{ii} + A_{ii})/C_{ii}\}^{1/2} \quad (1)$$

The natural uncoupled heave period for most free floating structures is in the range of 4 to 16 s [3]. The dominating exciting mechanism around this period is always linear. The restoring force for a buoy is due to the change in the buoyancy forces and is related to the water plane or wetted surface area. The uncoupled natural heave period of the buoy (T_{n3} = 4.2 s) was evaluated using a modified version of equation (1) as defined below:

$$T_{n3} = 2\pi \{(M + A_{33})/(\rho g A_w)\}^{1/2} \quad (2)$$

Table 1. Magnitudes and Nomenclatures of the Variables Used

Variable	Magnitude	Unit	Nomenclature
L	21.45	m	Length of buoy
B	16.5	m	Width of the buoy
A_w	353.925	m^2	Water plane area (L*B)
M	1,085,412	kg	Mass of the buoy
A_{33}	0.8M	kg	Heave added mass
A_{55}	-	N.m	Pitch added moment
A_{11}	-	kg	Surge added mass
GM_L	-	m	Longitudinal metacentric height
r_{55}	-	m	Pitch radius of gyration
O	-	-	Center of rotation of the buoy
W	-	-	Waterline of the buoy

The uncoupled natural period in pitch of the buoy is estimated from the following modified version of equation (1). The order of magnitude of T_{n5} (4.1 s) is similar to T_{n3}, the uncoupled natural heave period.

$$T_{n5} = 2\pi [\{M(r_{55})^2 + A_{55}\}/\{\rho g \blacktriangledown (GM_L)\}]^{1/2} \quad (3)$$

The uncoupled natural period for surge motion of the buoy was also estimated by the equation below:

$$T_{n1} = 2\pi \{(M + A_{11})/C_{11}\}^{1/2} \quad (4)$$

For a moored structure, like the buoy, the magnitudes of the uncoupled natural periods of surge, sway, and yaw are in minutes [3] and, therefore, too long compared to wave periods occurring under normal sea states. Thus, no noticeable uncoupled resonance surge response motion was seen in the results of the simulation.

2.1.2 Approach of the Computer Simulation

The hollow box-shaped buoy's wetted surface was discretized into 2 dimensional rectangular elements as shown in Figure 3.

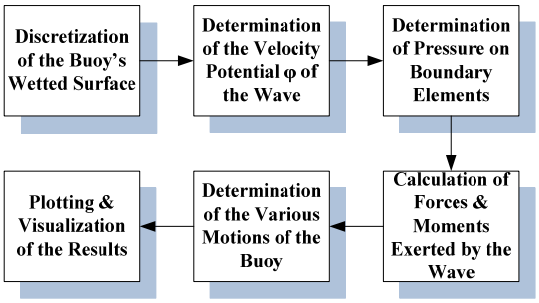

Figure 3. Outline of the Simulation Approach

Next, the velocity potential φ of the incident sinusoidal water waves, on infinite (100m) water depth, was determined. The dynamic pressure on the wetted surface was then found. Finally the wave loads and motion responses were evaluated.

2.2 3-D Sink-Source Method

Three dimensional Sink-Source technique was used to analyze the linear wave induced loads and resultant buoy motions. The technique has been extensively used in wave loading calculations for large volume structures like ships and offshore rigs [5].

In this method, differential equations representing a boundary value problem, were solved numerically using the Boundary Element Method. The concept of 3 dimensional sources over the discretized wetted surface was employed. The sources were considered as harmonically oscillating variables with zero mean speeds that generate 3 dimensional radiation wave fields. The source density, velocity potential, and fluid pressure were considered to be constant for each individual element.

2.3 Boundary Element Method

The determination of wave loads on and motion responses of the buoy was achieved using a well-established numerical computation technique known as Boundary Element Method. This method discretized the wetted surface continuum of the buoy into 2 dimensional quadrilateral elements. Each element was defined by a unique number (1 to 260) and four nodes (1 to 300). The nodes were shared between the elements to preserve continuity and transmit loads and motions. 2-D rectangular elements worked well as the buoy was assumed to be hollow as represented in Figure 4.

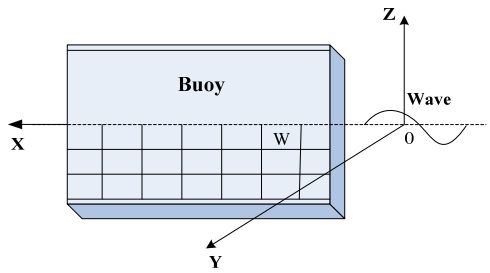

Figure 4. Discretization of the Buoy

The discretization resulted in a set of linear equations for the unknown source densities of the 6 DOF. The no-fluid-flow condition, through the wetted surface, was satisfied at the geometric center of each quadrilateral panel. Thus, the velocity, pressure, and all other subsequent calculations were performed at the geometric center of each element.

2.4 Computations

For the numerical computations of wave loads and buoy motions, the computer code, used for the calculations, was initially developed for wave force analysis on a box-shaped body. It was subsequently modified by Islam [5] for hydrodynamic interactions and drift force calculations of multiple floating structures.

The input to the program was from two sources. Initially the program received parameters from an input file. Once the program was compiled, built, and executed; the command prompt received user defined inputs for the incident wave periods. The outputs: wave loads, response motions, and phase angles were then generated.

3. RESULTS AND VALIDATIONS

The incident wave angle was taken to be 180° and fixed mooring conditions imposed on the buoy. It was assumed that the buoy was moored to the bottom of the sea bed by a cable of negligible weight. The mooring line prohibited any drift motion of the buoy. This condition resulted in making some of the wave loads and motion magnitudes zero or insignificant. Thus, the force F_y (sway), moments: M_x (roll) and M_z (yaw), and motions: Y (sway), Y_a (yaw), and R_a (roll) were insignificant. The noticeable parameters—forces: F_x (surge) and F_z (heave), moment M_y (pitch), and motions: X (surge), Z (heave), and P_a (pitch)—were non-zero as shown in Figures 5 to 9.

From Figure 5 it was observed that the surge motion of the buoy increased as the wave periods increased. The surge magnitude increased as the wave period was increased from 7 to 26 seconds. However, the increase in surge magnitude was steady and no sharp rises or peaks were observed. As already mentioned in the Discussion section, the uncoupled natural resonance period of a moored buoy is in minutes. Thus, no resonance motion was seen in normal sea states (wave periods from 7 to 26 s).

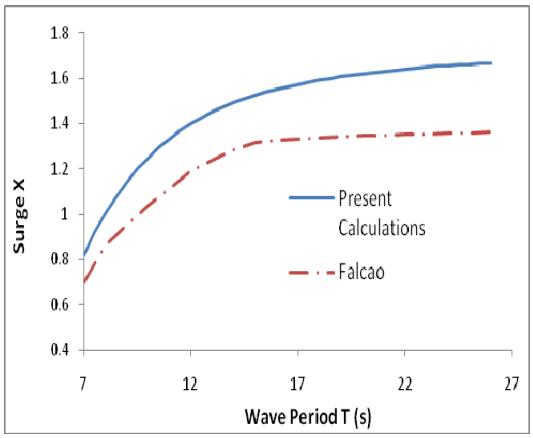

Figure 5. Surge Motion (X) of Buoy

A similar graphical result (chain-dot line with linear damping C = 2.5) was obtained by Falcao [2]. The discrepancy between the two results, Falcao's and the authors', resulted due to the fact that Falcao [2] modeled a rectangular buoy with a simple PTO whereas the authors did not include any PTO. Wave periods in the range of 7s to 26s were selected to be representative of normal sea states in North Atlantic (3.3 to 23.7 s) and North Pacific (5.1 to 22.5 s); Faltinsen [3].

The heave excitation force Fz for wave angular frequencies (ω) from 2.02 rads/s to 0.00001 rads/s was analyzed. This range for ω corresponds to wave periods from 3s to 628400s (T → ∞). The results obtained by the authors are represented in Figure 6 (dashed line). The results were compared with those obtained by Hong et al. [4] (solid line).

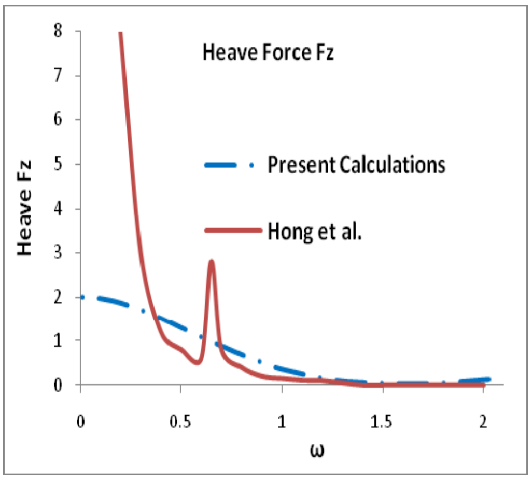

Figure 6. Heave Force (Fz) on Buoy

Hong et al. [4] obtained a resonance peak at 0.65 rads/s. This was due solely to the OWC and the

fluctuations smoothened with increasing equivalent linear damping . No such peak was therefore observed in the dashed curve as the authors did not model the OWC in the buoy.

The heave motion amplitude Z was analyzed and compared with the results obtained by Hong et al. [4] as represented in Figure 7.

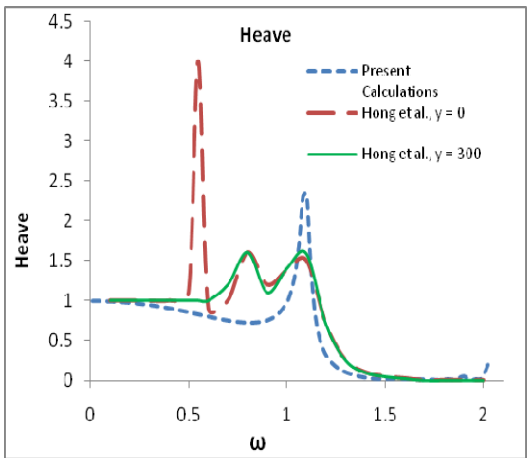

Figure 7. Heave Motion (Z) of Buoy

In Figure 7 the long dashes and solid line are results obtained for heave motion by Hong et al. [4]. They obtained different curves for two different linear damping conditions (long dashes for $\gamma = 0$ and solid line for $\gamma = 300$). The authors' results are represented by the small dashes in Figure 7. Again an OWC resonance peak was observed at $\omega = 0.56$ rads/s as shown in Figure 7 (long dashes). This was not seen in the authors' results as no OWC was modeled. The two other peaks, at $\omega = 0.85$ and 1.1 rads/s, in Figure 7 (long dashes and solid line), were due to the resonance of coupled surge-heave-pitch and uncoupled heave motions of BBDB-1 respectively. The authors obtained a similar coupled surge-heave-pitch resonance peak at a much higher frequency, $\omega = 1.1$ rads/s (Figure 7, small dashes). The authors' resonance peak's amplitude, due to uncoupled heave motion, was much smaller at 0.053 compared to Hong et al. [4] in Figure 7. It also occurred at a higher frequency, $\omega = 1.904$ rads/s compared to 1.1 rads/s in Hong et al. [4] model. The signs of another potential resonance peak, of coupled surge-heave-pitch motion, was detected around $\omega = 2.3$ rads/s, in the authors' results. However, this frequency was too high for normal sea state waves and hence, ignored.

The pitch motion P_a results were plotted as shown in Figure 8 (small dashes) and compared with the results obtained by Hong et al. [4] (Figure 8, solid line and long dashes).

In this case a similar OWC resonance peak was obtained at 0.56 rads/s (solid line), which was non-existent in the authors' results (small dashes). The resonance peak due to coupled surge-heave-pitch motion was also slightly shifted, to higher frequency, from $\omega = 0.85$ rads/s (Figure 8, solid line and long dashes) to $\omega = 1.1$ rads/s (Figure 8, small dashes).

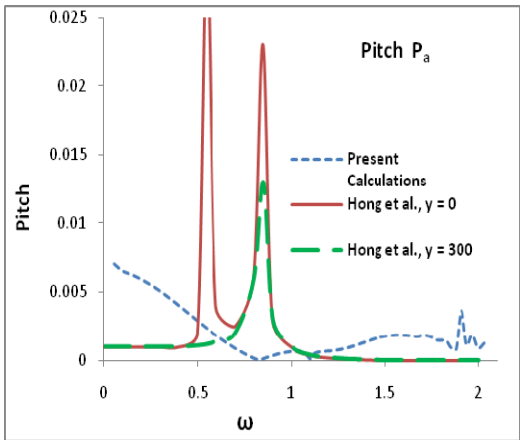

Figure 8. Pitch Motion (P_a) of Buoy

A second resonance peak, due to uncoupled pitch motion, was observed near $\omega = 2$ rads/s as shown in Figure 8 (small dashes). This agreed with the findings of Faltinsen [3] that the resonance frequency of heave and pitch uncoupled motions are similar in magnitude. A third resonance peak was observed near $\omega = 1.5$ rads/s as represented in Figure 8 by small dashes. This will be investigated further in subsequent research by the authors.

The pitch moment M_y was plotted as shown in Figure 9 by small dashes and evaluated against the results obtained by Hong et al. [4], also shown in Figure 9 by solid line ($\gamma = 300$) and long dashes ($\gamma = 0$).

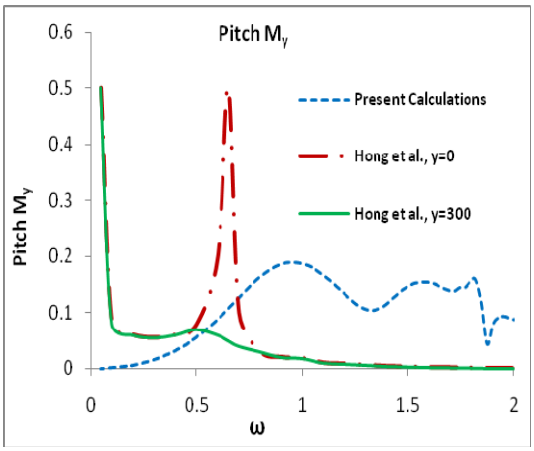

Figure 9. Pitch Moment (My) of Buoy

Hong et al. [4] obtained OWC resonance peak near $\omega = 0.65$ rads/s (Figure 9, long dashes) which was, as expected, non-existent in the authors' graph (Figure 9, small dashes). The authors, however, obtained the

forecasted coupled surge-heave-pitch resonance peak near ω = 1.1 rads/s (Figure 9, small dashes) and uncoupled pitch resonance peak near ω = 1.964 rads/s (Figure 9, small dashes). The third and fourth peaks, near ω = 1.6 and 1.8 rads/s (Figure 9, small dashes), require further investigation.

4. INFERENCES

The results of the numerical model and simulation were also compared against the previous seminal work of Islam [5] for further verification. The discrepancies between the results obtained by Hong et al. [4], Falcao [2] and the authors were attributed to different approximations and assumptions made in modelling. These discrepancies and the differences in modelling were addressed in the previous section.

The BBDB-1, modelled by Hong et al. [4] incorporated an open and submerged duct which was not present in the authors' buoy. The BBDB-1 also contained an OWC while the authors' buoy was considered to enclose a vacuum inside. The authors, unlike Hong et al. [4], also considered a moored buoy. These differences of geometry, inertia and relative movements of the OWC with respect to BBDB-1 inner walls account for the disparity between the two sets of results.

The rectangular buoy, modelled by Falcao [2], contained a simple linear damping PTO. Such a PTO was absent in the authors' model. Falcao [2], unlike the authors, did not consider mooring conditions. As a result, the disparity between the two sets of results was apparent in the graphical comparison.

The authors also modelled a moored buoy in order to make the ensuing calculations more amenable. The mooring acted against various motion modes of the buoy. These in-congruencies need to be studied more extensively prior to designing an efficient buoyant wave energy absorber.

5. CONCLUSIONS

As mentioned earlier, extensive research has been done on the behavior and motion of free floating buoys under varying conditions and assumptions. Special interests of the researchers have always been focused on the resonance response motion of such buoys. The results of the authors' simulation, adjusted for discrepancies caused by different initial assumptions, agreed with such established research observations regarding resonance motions

So, this computational model could be used to accurately determine the wave loads on and motion responses of a buoy of known dimensions, especially near the conditions of interest, i.e. resonance motion.

Admittedly, the model does have some inherent limitations, i.e. no wind loads, drift forces, or non-linear wave excitations were considered. The velocity potentials were evaluated at the panel elements' geometric centers. Hence, the model is less accurate in predicting parameters of interest near the elements' edges or at the buoy's sharp boundary corners. It was noted that the fluid flow actually separated at the sharp corners from the buoy's boundary surface. Consequently, the boundary element model has singularities at these regions. The handicap could be mitigated through the use of smaller dimension panel elements near the aforementioned corners.

However, the model and simulation results were accurate enough that, the model could be used in the optimal design of a Backward Bent Duct Buoy (BBDB) with an Oscillating Water Column (OWC); for the conversion of wave energy into electricity. The authors are of the opinion that their work will further the research in such renewable energy sectors.

ACKNOWLEDGEMENTS

The authors are grateful to the Faculty and Staff of Bangladesh University of Engineering and Technology (BUET) and Islamic University of Technology (IUT) for lending access to the institutions' computing facilities.

REFERENCES

[1] Duckers, L. J., "Wave energy: crests and troughs," *Renewable Energy,* Vol. 5, Part II, pp. 1444-1452 (1994).

[2] Falcao, AF de O., "Wave energy utilization: a review of the technologies," *Renewable and Sustainable Energy Reviews,* Vol. 14, pp. 899-918 (2010).

[3] Faltinsen, O. M., *Sea Loads on Ships and Offshore Structures,* U.K.: Cambridge University Press (1998).

[4] Hong, D. C., Hong, S. Y., and Hong, S. W., "Numerical study on the reverse drift force of floating BBDB wave energy absorbers," *Ocean Engineering,* Vol. 14, pp. 1257-1294 (2004).

[5] Islam, MR., "A study on motions and second order drift forces on multi-body floating system in waves," *Doctoral thesis,* Yokohama National University, Japan (2001).

[6] Masuda, Y., "Wave-activated generator," *International Colloq Exposition Oceans,* France: Bordeaux, (1971).

[7] McCormick, M. E., *Ocean Wave Energy Conversion*, New York: Wiley *(*1981).

[8] Shaw, R., *Wave energy: a design challenge,* Chichester: Ellis Horwood *(*1982).

[9] Slater, SH., "World progress in wave energy," *International J. Ambient Energy,* Vol. 10, pp. 3-24 (1989).